Properties of High Density Polyethylene – Paulownia Wood Flour Composites via Injection Molding

Brent Tisserat,[a,*] Louis Reifschneider,[b] Nirmal Joshee,[c] and Victoria L. Finkenstadt [d]

Paulownia wood (PW) flour was evaluated as a reinforcement for thermoplastic composites. Composites of high-density polyethylene in pellet form (HDPE), 25% by weight of PW, and either 0% or 5% by weight of maleated polyethylene pellets (MAPE), were produced by twin screw compounding followed by injection molding. Formulations of PW flour composed of specific particle sizes (≤590 to ≤75 µm) were also compared. Molded test composites were evaluated for their tensile, flexural, impact, and thermal properties. Composites made with PW and MAPE had significantly improved tensile and flexural properties compared to neat HDPE. The impact strength of all composites using MAPE was 30% improved over HDPE. Benchmarking PW composites to similar preparations of pine wood flour composites demonstrated that PW can produce a comparable and in some cases a superior bio-fiber composite. The effect of environmental exposure was examined by soaking tensile bars of HDPE-PW blends in distilled water for 28 days to observe changes in their physical and mechanical properties. Finally, differential scanning calorimetery and thermogravimetric analysis were conducted on PW composites to evaluate their thermal properties and the implications these may have on selecting processing conditions for the bio-fiber reinforcements.

Keywords: Particle size; Adsorption tests; Mechanical properties; Flexural properties; Colorimetery; Differential scanning calorimetry; Thermal properties

*Contact information: a: Functional Foods Research Unit, National Center for Agricultural Utilization Research, Agricultural Research Service, United States Department of Agriculture, 1815 N. University St., Peoria IL 61604 USA; b: Department of Technology, College of Applied Science and Technology, Illinois State University, Normal IL 61790-5000 USA; c: Agricultural Research Station, Fort Valley State University, Fort Valley, GA 31030 USA; d: Plant Polymer Research Unit, National Center for Agricultural Utilization Research, Agricultural Research Service, United States Department of Agriculture, Peoria, IL 61604 USA; *Corresponding author: Brent.Tisserat@ars.usda.gov*

INTRODUCTION

The most common type of lignocellulosic plastic composite (LPC) is the wood plastic composite (WPC), which utilizes wood flour (WF) fillers derived from wood waste materials such as shavings and sawdust generated from lumber processing (Carlborn and Matuana 2006; Lei *et al*. 2007; Clemons 2010; Zahedi *et al*. 2012). WPC thermoplastics typically include polyethylene (PE), polypropylene (PP), and polystyrene and are mixed with up to 50% WF (w/w) depending on the desired mechanical and physical properties and industrial acceptance (Carlborn and Matuana 2006; Lei *et al*. 2007; Clemons 2010). The U.S. WPC industry is projected to increase 13% a year to amount to $5.3 billion in 2015 and is likely to continue to increase at the same rate in the foreseeable future (Anonymous 2012). There is a great interest in the development of

improved WPC with high durability and lower costs than existing products (Berglund and Rowell 2005; Carlborn and Matuana 2006; Clemons and Stark 2009; Zahedi *et al.* 2012; Ashori *et al*. 2013). The price of WPC is dictated by the price of petroleum and the cost of wood fillers. Wood waste material prices fluctuate on the basis of availability (housing demand) and the demand for their utilization (Millman 2008). For example, between 2006 and 2008, when the US housing market contracted, sawdust prices quadrupled due to a lack of supply (Millman 2008). Currently, 85% of wood waste is consumed for energy production (fuel pellets and direct combustion) (Burden 2012). The Energy Independence and Security Act of 2007 mandates that 36 billion gallons of biofuels be produced by 2022 and woody biomass materials will be increasingly utilized to achieve this goal (Eilperin 2010). A number of government subsidy programs are already diverting the sale of woody biomass to bio-energy facilities. Changes in the cost, availability, and utilization of the biomass and wood waste markets are occurring (Eilperin 2010). Since the demand for WF needed by the WPC industry will also increase and the cost of WF will undoubtedly increase due to the bio-energy mandates, new sources of woody biomass are clearly needed.

Alternative woody biomass sources to provide WF are being developed (LeVan-Green and Livingston 2001; Myers *et al*. 2003; Stark and Mueller 2008; Clemons and Stark 2009). Harvesting small-diameter trees obtained from forest under-stories or brush conditions offers a source of wood waste materials for both bio-energy as well as WF for WPC (LeVan-Green and Livingston 2001; Myers *et al*. 2003). Short-rotational woody crops utilizing "fast-growing trees" are another option to obtain woody waste materials (English and Ewing 2002). Marginal land utilization has been suggested as the potential site for planting large acreages of bio-energy woody tree crops (English and Ewing 2002; Berglund and Rowell 2005; Bevill 2011).

Paulownia elongata S. Y. Hu, family Paulowniaceae, a native to China, is an extremely fast-growing coppicing hardwood that is cultivated in plantations in China and Japan. Paulownia wood is highly valued in the construction and furniture industries (Chinese Academy of Forestry Staff 1986; Anonymous 2011). A Paulownia plot containing 2000 trees per hectare and can yield up to 150 to 300 tons of wood within 5 to 7 years (Joshee 2012). Growth rate of heights up to 3.7-4.6 m and diameters of 3 to 5 cm a year are common (Anonymous 2011; Joshee 2012). Paulownia trees are amenable to being established on marginal lands and have deep taproots, which make them drought resistant (Anonymous 2011). Characteristics of Paulownia wood (PW) include: light weight, insect resistance, pale coloration, and heat resistance (Chinese Academy of Forestry Staff, 1986; Ashori and Nourbakhsh 2009; Anonymous 2011; Joshee 2012). Paulownia species such as *P. elongata*, *P. kawakamii*, and *P. tomentosa*, are currently being grown and evaluated in the United States for their commercial wood properties (Anonymous 2011; Joshee 2012). Recent studies conducted at Fort Valley State University, Fort Valley, GA show that two to four-year-old trees can grow to a diameter of 16.5 cm and achieved a height of 10 m. Such trees offer an inexpensive source of woody biomass for energy and lumber, which will provide the wood wastes needed to manufacture WF (Ashori and Nourbakhsh 2009; Joshee 2012).

Because there have been relatively few studies of the use of Paulownia wood as a fiber reinforcement for thermoplastics (Zahedi *et al.* 2012; Ayrilmis and Kaymakci 2013), the objective of this study was to evaluate the mechanical, physical, and thermal properties of WPC obtained from blending Paulownia wood flour (PWF) with high density polyethylene (HDPE). There is particular interest in the utilization of PWF

derived from juvenile trees since small diameter short-rotation woody crop trees are likely to be a source of woody biomass needed by the US in the future. Hence, this study was conducted utilizing PWF derived from juvenile tree biomass (*i.e.*, 36-month-old). Coupling agents have been commonly used for wood fiber PE composites (Carlborn and Matuana 2006; Lei *et al*. 2007; Clemons 2010; Zahedi *et al*. 2012), so the use of a maleated PE was employed as part of the scope of the project. Further, because particle size may affect the performance of reinforcement, the mechanical and flexural properties of WPC derived from PW utilizing different sized particles were examined. The mechanical and flexural properties of PW were benchmarked to comparably formulated pine wood (PINEW) flour composites and neat HDPE to demonstrate how PW compares to an established WF reinforcement. The mechanical property outcomes were normalized to the control HDPE for ease of assessing the benefit of various filler treatments. Because PW is a bio-filler and is subject to degradation by water, water immersion tests were administered on these PWF composites to evaluate their environmental durability. Finally, differential scanning calorimetry and thermogravimetric analysis were conducted on PW composites to evaluate their thermal properties and the implications these may have on selecting processing conditions for the bio-fiber reinforcements.

EXPERIMENTAL

Materials

The resin matrix material was high-density polyethylene (HDPE) (Petrothene LS 5300-00, Equistar Chemicals LP, Houston, TX). The HDPE had a melt-flow index of 40 g/10 min, a density of 0.950 g/cm^3, and a melting point of 129 ^{o}C. The binding agent was a polyethylene-graft-maleic anhydride, or maleated polyethylene (MAPE), (Product code NE542013, Equistar Chemicals LP). It had a melting point of 104-138 ^{o}C with approximately 1% maleic anhydride by weight grafted on the polyethylene.

Paulownia elongata wood material was obtained from 36-mo-old trees grown in Fort Valley, GA. PW shavings were milled successively through 4-, 2-, and then 1-mm screens with a Thomas-Wiley mill grinder, (Model 4, Thomas Scientific, Swedesboro, NJ). Particles were then sized through a Ro-Tap^{Tm} Shaker (Model RX-29, Tyler, Mentor OH) employing 203 mm diameter stainless steel screens. Screens employed were #10, #30, and #40 US Standards (Cole-Parmer/ ThermoFisher Scientific, Waltham, MA). The PW mixtures consisted of ≤590 µm particles obtained from particles passing through the #30 mesh sieve and particles collected by the successive sieves were designated as #40 mesh and finer (≥#40), thereafter. White pine (*Pinus strobus* L.) shavings were treated in the same manner as PW material to produce pine wood (PINEW) flour material (American Wood Fiber, Schofield, WI). Ball ground PW (BGPW) flour was obtained from 1-mm milled PWF and ground in a laboratory bench top ball mill (Model 801CVM, U.S. Stoneware, East Palestine, OH) to obtain fine powder. PWF was ground in alumina mill jars containing Burundum cylindrical grinding media pellets (13 mm diam, ≈7.3 g wt.) (U.S. Stoneware) at a speed of 50 rpm for 60 h. BGPW flour was sieved through a #200 screen and designed hereafter as finer than #200 mesh (>#200) and to be composed of ≤75 µm particle sizes. Each screened fraction was oven dried for 48 h at 100 ^{o}C to obtain a moisture content of ~1 to 2%.

Preparations

Sample preparations of the various PW and PINEW composites are summarized in Table 1.

Table 1. Weight Percentages in Test Formulations

Composition	PW (≥#40)	PW (>#200)	PINEW (≥#40)	MAPE	HDPE
HDPE	--	--	--	--	100%
HDPE-MAPE	--	--	--	5%	95%
HDPE-25BGPW	--	25%	--	--	75%
HDPE-25BGPW-MAPE	--	25%	--	5%	70%
HDPE-25PW	25%	--	--	--	75%
HDPE-25PW-MAPE	25%	--	--	5%	70%
HDPE-40PW	40%	--	--	--	60%
HDPE-40PW-MAPE	40%	--	--	5%	55%
HDPE-25PINEW	--	--	25%	--	75%
HDPE-25PINEW-MAPE	--	--	25%	5%	70%

Composite blends were extruded with a Micro-18 30/l L/D co-rotating twin-screw extruder (American Leistritz Extruder, Branchburg, NJ). The barrel had six different zones, each 90 mm long, which were controlled at the following temperatures (^{o}C): 30, 60, 90, 125, 135, and 140, respectively. The strand die temperature was set at 138 ^{o}C. The HDPE and MAPE used were in pellet form. The PW and PINEW were in the form of wood flour.

Premixed weight fractions of PW or PINEW with MAPE were fed into zone 1 at ~4.4 g/min using a volumetric twin-screw gravimetric feeder (Model KCL24KT20, Ktron, Pitman, NJ). At the same time, HDPE was fed with a single drive feeder (Flex-Tuff Model 106, Schenck/AccuRate, Whitewater, WI) in the same zone at the rate of ~12 g/min. Extruder screw speed was set at 100 rpm. Extruded strands were cooled on a conveyor belt equipped with an air stream (Model 2100, Dorner Mfg. Corp., Hartland, WI) and were processed into pellets with a strand pelletizer (Model 4, Killion, Cedar Grove, NJ).

An ASTM test specimen mold was used that included cavities for a ASTM D790 flexural tensile bar (12.7 mm W × 127 mm L × 3.2 mm thickness), an ASTM D638 Type I tensile bar (19 mm W grip area × 12.7 mm neck × 165 mm L × 3.2 mm thickness x 50 mm gage L), and an ASTM D638 Type V tensile bar (9.53 mm W grip area × 3.18 mm neck × 63.5 mm L × 1.5 mm thickness x 7.62 mm gage length). Impact specimen bars were obtained by cutting the flexural specimens in half to 12.7 mm W × 64 mm L × 3.2 mm thickness and notched.

Molding was conducted with a 30-ton molding machine (Engel ES 30, Engel Machinery Inc., York, PA) with set point temperatures (°C) for the four zone injection molding barrel set at: feed = 160; compression = 166; metering = 177, and nozzle = 191. The mold temperature was 37 °C.

Mechanical Property Measurements

Samples were conditioned for approximately 240 h at standard room temperature and humidity (23 °C and 50% RH) prior to any test evaluations. ASTM D638 Type I tensile bars were tested for tensile modulus and strength using a universal testing machine (UTM) (Model 1122, Instron Corporation, Norwood, MA). The speed of testing was 50 mm/min, which is 1 mm/mm/min strain rate at the start of the test.

Three-point flexural tests were carried out according to ASTM D790 specification on an Instron UTM (Model 1122). The flexural tests were carried out using Procedure B with a rate of straining of the outer fiber equal to 0.1 mm/mm/min. In addition, there was a slight modification in the maximum allowed bending strain because Procedure B failed to achieve a maximum bending force within the 5% strain limit; the maximum bending occurred between 5.5 to 8% of strain. The flexural strength σ_{fM} and the modulus of elasticity in bending E_b were calculated using the following formulas,

$$\sigma_{fM} = 3PL/2bd^2 \quad (1)$$

$$E_b = L^3m/4bd^3 \quad (2)$$

where P is the maximum applied load, L is the length of support span which was 50.8 mm, m is the slope of the tangent of the load to deflection curve, and b and d are the width and thickness of the specimen bars, respectively.

Notched impact tests were conducted with an IZOD impact tester, Model Resil 5.5, P/N 6844.000 (CEAST, Pianezza, Italy) conformed to ASTM D256-84.

Water Absorption

The Type V tensile bars injection molded for each composite were dried in an oven for 24 h at 100 ± 2 ^{o}C and weighed. Tests were conducted in an incubator at 25 ± 2 ^{o}C under a photosynthetic photon flux density of 180 $\mu mol \cdot m^{-2} \cdot s^{-1}$ using a photoperiod of 12 h light/12 h dark. Tensile bars were placed in distilled water at room temperature for 672 h. At predetermined time intervals the specimens were removed from the distilled water, the surface water was blotted off with paper towels, and their wet masses were determined. Water absorption, measured as weight gain percentage, was computed using the following formula,

$$\text{Weight gain (\%)} = (m_t - m_o)/m_o \times 100 \quad (3)$$

where m_o denotes the oven-dried weight and m_t denotes the weight after soak time t.

Thermal Properties

Differential scanning calorimetry (DSC) of molded specimens was conducted with an Auto DSC-7 calorimeter with a TAC/DX controller (TA Instruments, New Castle, DE). Samples of 5 to 7 mg were weighed and sealed hermetically in aluminum DSC pans. First, the calorimeter was programmed to increase the temperature from 0 to 180 ^{o}C at a rate of 10 ^{o}C/min, kept isothermal for 3 min. Second, the samples were cooled to -50 ^{o}C at a rate of 10 ^{o}C/min. Finally, the samples were heated to 180 ^{o}C from -50 to 180 ^{o}C at the same rate. Data from the second heating cycle were used to determine the melting temperature (T_m) and enthalpy of melting (ΔH_m) for PE-PW blended samples.

Data from the second cooling cycle were used to determine the crystallization temperature (T_c) and crystallization enthalpy (ΔH_c) for the same samples. The heat flow rate corresponding to the crystallization of HDPE in composites was corrected for the content of the WF and MAPE. The value of crystallization heat was also corrected for the crystallization heat of MAPE. The degree of crystallinity (χ_c) of the HDPE matrix was evaluated from the following relationship (Lei *et al.* 2007),

$$\chi_c = \Delta H_{exp}/\Delta H \times 1/W_f \times 100\% \quad (4)$$

where ΔH_{exp} is the experimental heat of fusion (ΔH_m) or crystallization determined by DSC, ΔH is the assumed heat of fusion or crystallization of fully crystalline HDPE (293 J/g), and W_f is the weight fractions of HDPE in the composites.

Thermogravimetric analysis (TGA) was performed to determine the thermal characteristics of the composites. TGA was conducted using a Model 2050 TGA (TA Instruments) under nitrogen at a scan rate of 10 ^oC/min from room temperature to 600 ^oC. A sample of ~7.5 mg was used for each run. Data were analyzed using the TA Advantage Specialty Library software (TA Instruments). The derivative TGA (wt %/min) of each sample was obtained from the software.

Statistical Analysis

Five specimens of each formulation were tested in the mechanical, flexural, and impact strength tests. The average values and their standard errors were reported. Experimental data obtained was analyzed statistically by analysis of variance for statistical significance, and multiple comparisons of means were accomplished with Duncan's Multiple Range Test ($p \leq 0.05$).

RESULTS AND DISCUSSION

Mechanical Properties

The mechanical properties of tensile strength (σ_U), Young's modulus (E), and elongation at break (%El) of the biocomposites containing various PW and PINEW formulations are shown in Table 2. Figure 1 graphically summarizes the data in Table 2 by normalizing the outcomes to the HDPE control material. For example, the σ_U of HDPE-MAPE is 96% of the neat HDPE, thus the bar graph of the normalized σ_U for HDPE-MAPE is 96%. This rendering clearly illustrates the effect of various additives.

The first comparison shown is the effect of wood fiber on the composite's tensile strength. Tensile strength is a measure of a material to support a stress load without generating voids that leads to crazing of the material and ultimate failure. The tensile strength values for PW and PINEW composites made without the MAPE coupling agent were comparable to neat HDPE; refer to Table 2 and Fig. 1. Other studies have shown this trend (Girones *et al.* 2007, Karmarkar *et al.* 2007). Inclusion of a MAPE with HDPE enhanced the tensile strength of the PW and PINEW composites by almost 50%. The increase in tensile strength is attributed to better transfer of stress between the hydrophobic wood fiber and the hydrophilic HDPE matrix due to the chemical coupling. The improved surface contact between the wood and the HDPE also leads to fewer

locations for microscopic cracks to form and this retards failure due to crack formation which limits tensile strength.

Table 2. Tensile Mechanical Properties of Composites*

Composition	σ_U (MPa)	*E* (MPa)	%El (%)
HDPE	21.5 ± 0.1a	339 ± 10a	105 ± 5a
HDPE-MAPE	20.5 ± 0.2b	333 ± 15a	103 ± 2a
HDPE-25BGPW	20.4 ± 0.2b	563 ± 5b	11 ± 0.5b
HDPE-25BGPW-MAPE	27.4 ± 0.5c	597 ± 20c	12 ± 1b
HDPE-25PW	21.2 ± 0.1d	689 ± 20d	8 ± 0.3c
HDPE-25PW-MAPE	31.3 ± 0.1e	696 ± 16d	13 ± 0.2b
HDPE-40PW	21.6 ± 0.2a	872 ± 24e	5 ± 0.1e
HDPE-40PW-MAPE	35.6 ± 0.4f	925 ± 19e	9 ± 0.2f
HDPE-25PINEW	20.2 ± 0.1b	640 ± 5f	11 ± 0.1b
HDPE-25PINEW-MAPE	29.9 ± 0.1g	680 ± 7g	15 ± 0.2g

*Treatment values with different letters in the same column were significant ($P \leq 0.05$). Means and standard errors derived from five different replicates are presented.

The inclusion of 25% bio-fiber reinforcements dramatically improved the elastic modulus. This improvement was due to the presence of the stiffer wood particles that impeded the deformation of the spherulites in the matrix. Modulus is a low deformation mechanical property that is not affected by poor adhesion of the filler with the matrix. Consequently, when MAPE is added, there is relatively little increase in stiffness over the already improved modulus. The third property summarized in Table 2 and Fig. 1 is the percentage elongation at break in tension, which is largely a deformation property. The percent elongations to break for all the wood composites were much lower than the neat HDPE. Any reduction in the adhesion of material at the matrix/composite interface provides a location for a microscopic crack to form. This leads to crazing within the matrix and subsequent failure at relatively low elongations. The addition of MAPE helped improve the elongation by a modest amount, but apparently there were still numerous locations where the discontinuity of the hydrophobic wood fiber and the hydrophilic HDPE existed.

The HDPE-25PW composite yielded comparable tensile strength and elastic modulus results to the HDPE-25PINEW composite. This suggests that paulownia wood, PWF, is at least equivalent to pine, PINEW flour, which is commonly employed in WPC. Finally, the relatively labor intensive ball ground filler, HDPE-25BGPW, was not found to be superior to the HDPE-25PW composite. The modulus of the ball ground composite, 25BGPW, is less than the milled wood, 25PW. This is attributed to the high percentage of small particles in the ball ground filler (≤74 μm) compared to the broad range of particles found in the ≥#40 mesh PW flour (25PW), which also contains larger particles (≤590 μm). The larger particles impede the deformation of the spherulites. In a similar way, the 40% loading of PW, 40PW, exhibited a higher modulus than the 25% loading. In addition, the tensile strength of the ball ground composite was no different than the ≥#40 mesh flour when no MAPE was used and not as great as the more course 25PW when MAPE is used. This trend is likely related to the relative surface area of the ball ground filler compared to the ≥#40 mesh flour. As the particle size of a filler was decreased with

the mass loading remaining the same, the surface area inversely increased. Consequently, the ball ground filler had more interfacial area of the incompatible wood to HDPE than the 25PW and thus has a greater number of locations at which cracks can form that will limit the tensile strength.

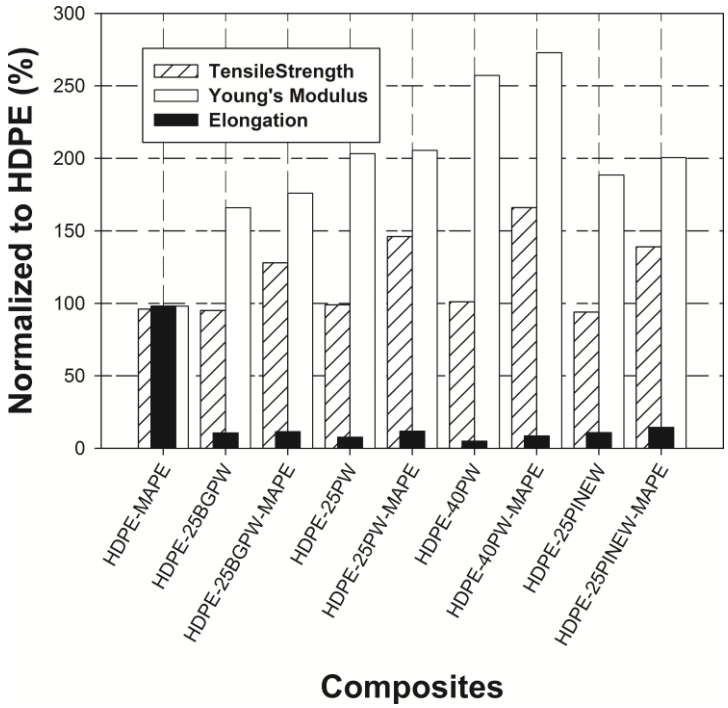

Fig. 1. Effect of additives on the tensile mechanical properties when compared to the control material HDPE

Flexural Behavior

The flexural strength (σ_{fM}) and flexural modulus or modulus of elasticity in bending (E_b) of the composites and thermoplastic resins are given in Table 3. Figure 2 illustrates the effect of the additives compared to HDPE. As with the tensile properties, the PW composite yielded comparable flexural properties to the PINEW composite. In fact, there was a greater proportional improvement in the flexural strength of the PW composite than the PINEW with the addition of MAPE. The strength property is related to the composites ability to transfer a stress load without creating microscopic cracks. The MAPE improves the interfacial bonding of the wood fiber and the HDPE, which explains why the strength values increased for the PW and the PINEW composites. However, the flexural modulus values, unlike those for pure tension, did exhibit a change with the addition of MAPE. This is attributed to the fact that flexural loading involves both tensile and compressive stress fields. During a flexural load, two unique modes of stress transfer are at play. On the tensile side of the specimen there is a stress transfer without creating micro cracks that depends upon good adhesion. On the compressive side of the specimen there is a stress build-up by impeding the deformation of spherulites that does not depend so much on good adhesion of the filler to the matrix. Further, there is likely a shape factor affecting the results seen in Table 3 for the flexural strength and flexural modulus because there is not a discernible correlation of strength and modulus. There have been other studies done (Ehrenstein 2001) utilizing short glass fibers and

glass spheres as reinforcements in thermoplastics that show glass spheres lowering strength values but improving both flexural and tensile moduli. The short glass fiber, conversely, improved all strength and moduli values.

Table 3. Flexural and Impact Properties of HDPE and Composites*

Composition	σ_{fM} (MPa)	E_b (MPa)	Impact Strength (J/m)
HDPE	27.9 ± 0.1a	894 ± 15a	38.7 ± 0.7a
HDPE-MAPE	26.1 ± 0.1a	804 ± 8b	38.6 ± 0.6a
HDPE-25BGPW	51.2 ± 0.2c	1384 ± 15d	39.4 ± 0.5a
HDPE-25BGPW-MAPE	48.7 ± 1.2b	2365 ± 118c	50.6 ± 0.9b
HDPE-25PW	35.0 ± 0.3d	1865 ± 38i	36.5 ± 0.9a
HDPE-25PW-MAPE	62.8 ± 0.3e	1638 ± 28f	51.8 ± 1.3b
HDPE-40PW	24.7 ± 0.1f	1049 ± 7g	36.5 ± 0.9a
HDPE-40PW-MAPE	67.8 ± 4.1g	2809 ± 128h	53.9 ± 1.4b
HDPE-25PINEW	32.6 ± 0.1h	1810 ± 16j	39.3 ± 0.5a
HDPE-25PINEW-MAPE	43.7 ± 0.1i	1814 ± 14i	50.3 ± 1.0b

*Treatment values with different letters in the same column were significant ($P \leq 0.05$). Means and standard errors derived from five different replicates are presented.

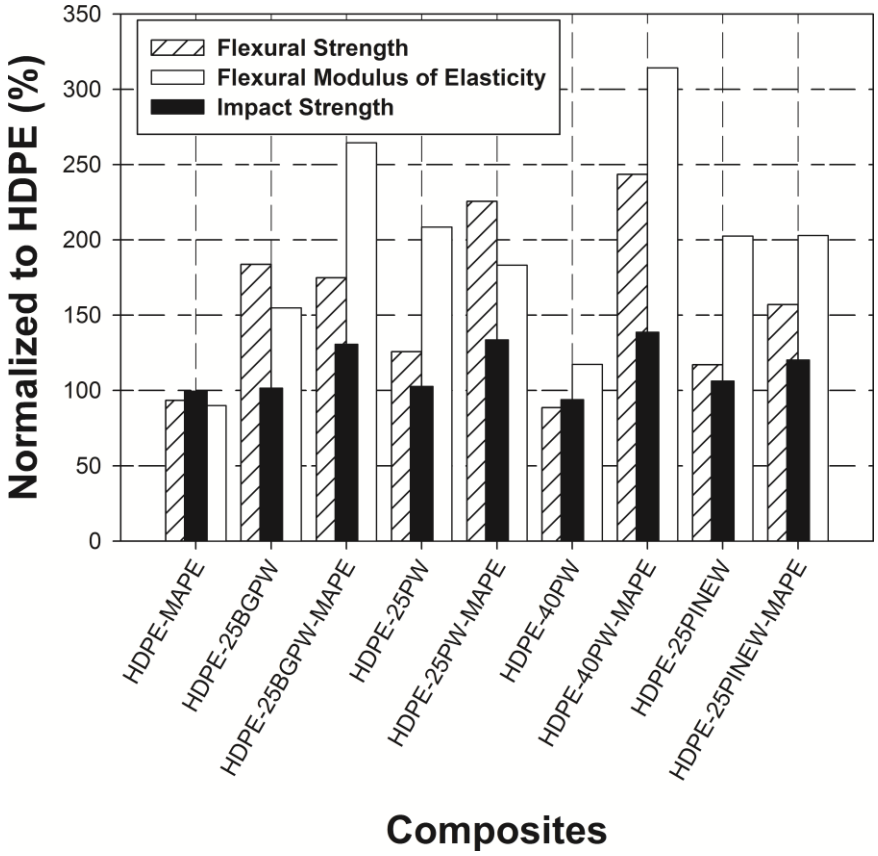

Fig. 2. Effect of additives on the composite's flexural strength, flexural modulus of elasticity, and impact strength properties compared to the control material HDPE

Impact Strength

The notched IZOD impact strength for the various composites is listed in Table 3. The inclusion of filler with the coupling agent (MAPE) increased the impact strength of the composites by almost 40%. However, even when a coupling agent was not included, the composite impact strength was comparable to neat HDPE. Some studies have shown that notched IZOD impact strength generally decreases with increasing filler content (Stark and Berger 1997; Ayrilmis and Kaymakci 2013). However, other researchers have found that wood fiber polypropylene composites exhibit no reduction in notched IZOD impact strength compared to the neat thermoplastic as the filler content increases (Hristov *et al*. 2004; Ramaraj 2007; Karmarkar 2007). Also, contrary to this study, Myers *et al*. (1991) found that inclusion of MAPE had a negative effect on notched impact strength of pine WPC compared to those specimens without MAPE. The observed differences may be due to the different source of fillers, different matrices HDPE *vs*. PP, and the coupling agent employed, making discrepancies in comparisons difficult to resolve.

An apparent anomaly exists when comparing the dramatic reduction in the percentage elongation at break of the composites to the fact that the composites exhibit improved impact strength compared to the neat HDPE. However, this trend has been seen in other studies involving biofiber/polypropylene composites (Hristov *et al*. 2004; Ramaraj 2007). The elongation to break is a relatively slow and large deformation process that is sensitive to the initiation of cracks at the incompatible material interface of the wood fiber and HDPE. On the other hand, the impact property is a dynamic phenomenon that depends upon several factors.

The impact strength measured in this study involved the propagation of a crack due to an existing notch. There are several mechanisms that affect the energy dissipated during crack propagation (Thomason and Vlug 1997): plastic deformation of the matrix in front of the crack tip, fiber debonding from the matrix, and fiber breakage and pull-out from the matrix. Another factor is called crack pinning, where a fiber holds the matrix together as the crack advances because the fiber is either chemically bonded or mechanically linked to the matrix.

The plastic deformation of the matrix in the area in front of the propagating crack can be influenced by the degree of crystallinity present in the matrix. The DSC data in this study, Table 5, shows there is a significant reduction in the degree of crystallinity present in the matrix as wood fiber is added. Also, the addition of MAPE further lowers the degree of crystallinity. It is known that a higher percentage of crystallinity in a semi-crystalline polymer will lower the impact energy (Xu *et al.* 2001). Thus, one mechanism to account for this apparent anomaly is that the wood fiber composite lowers the degree of crystallinity that corresponds to a greater mass of amorphous HDPE that can plastically deform, as opposed to brittle fracture, and thus absorb more energy during crack propagation.

The fact that MAPE is shown to improve the impact strength is attributed to the increased energy required to debond the wood fiber from the matrix. The scope of this study did not include the use of SEM to document the role of fiber pullout in the impact data. Therefore, a combination of effects may account for the apparent discrepancy between the %El data and the IZOD impact data. These are the change of degree of crystallinity effects, fiber crack-pinning, and in the case of MAPE, debonding of fiber with the matrix.

Water Absorption Responses

Figure 3 shows the long-term water absorption plots of PW-based composites at room temperature, where weight gain (%) (*i.e.* water absorption) is plotted against immersion time (h). HDPE and HDPE-MAPE did not increase in weight after the immersion incubation time. Inclusion of the MAPE coupling agent to the formulation generally produces a composite that is more resistant to water absorption. Both untreated HDPE-PW treatments (25PW and 40PW without coupling agent MAPE) exhibited higher weight gains than those PW composites with coupling agents (MAPE), as seen in Fig. 3. For example, at the end of 672 h, the composite composed of HDPE-25PW blends increased by 3.8% in weight while the composite of HDPE-25PW-MAPE exhibited only a 1.8% increase in weight (≈100% less increase). This observation confirms findings previously reported by others, who have found that inclusion of MAPE in the composite considerably reduces water absorption when using bio-fillers of popular wood, loblolly pine wood, sisal fiber, or wheat straw (Joseph *et al.* 2002; Zabihzadeh 2010). This can be attributed to the covalent binding of the anhydride groups in the MAPE to the hydroxyl groups of the PWF, which results in a composite that has less space in its interfacial regions to be subjected to water (Zabihzadeh 2010). It is interesting that HDPE-BGPW composed of smaller particles (≤75 μm) exhibited considerably less weight gain (2.4%) than HDPE-25PW (4%) or 40PW (7.2%), which contained larger particles (≤590 μm). However, when MAPE was included into the formulation, no difference was found in weight change values for the HDPE-BGPW-MAPE and HDPE-25PW-MAPE formulations (see Fig. 3 and Table 4).

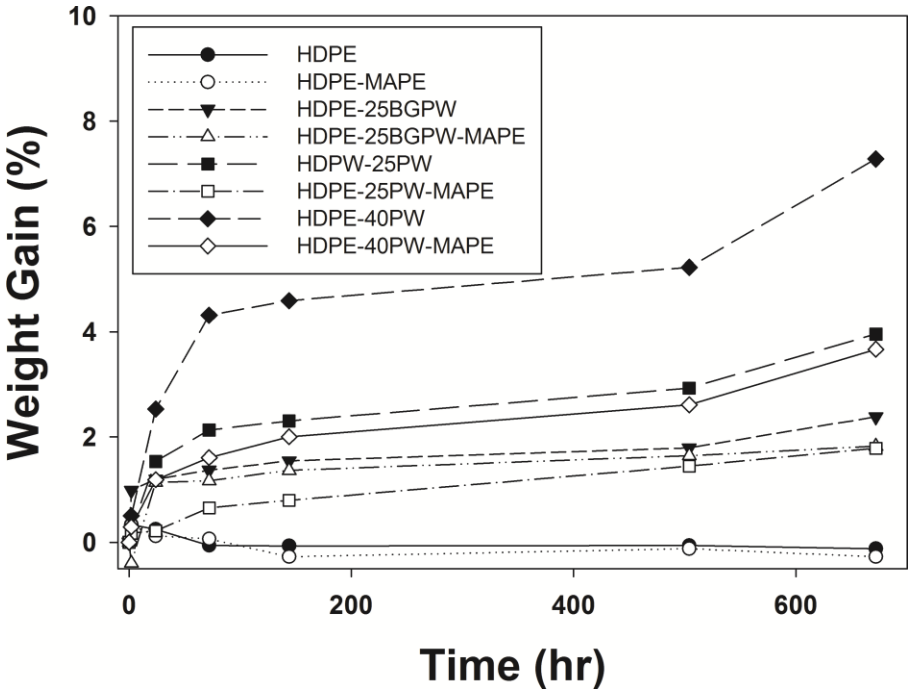

Fig. 3. Comparative water absorption plots for various PW composites over 672 h of soaking

The response of biocomposites to water soaking is related to the bio-filler's chemical and lignocellulosic anatomical properties (Joseph *et al.* 2002; Zabihzadeh 2010). Clearly, addition of higher PW filler concentrations (*i.e.*, 40PW) resulted in a

composite that was less resistant to water soaking as evidenced by its ability to gain weight. Absorption of water by composites is a crucial factor in the determination of the ability of biocomposite to be commercially utilized (Zabihzadeh 2010). However, as previously noted, less weight gain occurred in this composite if a coupling agent was employed, which indicates that additives will much improve the performance of composites to environmental stresses.

Environmental stresses such as water soaking may cause changes in the mechanical properties to occur, which needs to be measured in order to assess the potential commercial value of a composite (Thwe and Liao 2002; Lopez *et al.* 2006; Clemons and Stark 2009; Zabihzadeh 2010). For example, flexural properties have been reported to decrease when lignocellulosic plastic composites are weathered (Thwe and Liao 2002; Lopez *et al*. 2006; Clemons and Stark 2009). In this work, the Type V tensile bars that were not soaked and Type V bars that were soaked in water for 672 h were tested for their mechanical properties, as shown in Table 4. Soaked HDPE and HDPE-MAPE blends exhibited reductions in elongation to breaking values while the values for tensile strength and tensile modulus increased slightly. Tensile strength values increased about 4 and 6% for HDPE and HDPE-MAPE, respectively. The tensile strength values for soaked composites were either retained (*i.e.,* HDPE-25BGPW-MAPE, HDPE-25PW, HDPE-40PW-MAPE) or increased (*i.e.,* HDPE-25BGPW, HDPE-25PW-MAPE, HDPE-40PW). Young's modulus values also varied in the blends. In some blends, E-values declined (*i.e.,* HDPE-25BGPW-MAPE, HDPE-40PW, HDPE-40PW-MAPE), and in other blends E-values were retained (*i.e.,* HDPE-25BGPW, HDPE-25-MAPE) when compared to untreated controls (Table 4; Fig. 4). The largest change in tensile values occurred in the HDPE-BGPW composite, which increased 8%. The HDPE-40PW-MAPE composite still retained the highest σ_U and E-values when compared to HDPE, HDPE-MAPE, or other composite formulations (Table 4). ELO values varied less than other mechanical properties examined when comparing the soaked composites with the unsoaked composites.

Table 4. Mechanical Properties of Original and Soaked Type V Tensile Bars

	σ_U (MPa)		*E* (MPa)		%El (%)		Wt. Gain %
Composition	Original	Soak	Original	Soak	Original	Soak	
HDPE	18	19*	152	160*	1716	1014*	-0.1
HDPE-MAPE	17	18*	149	158*	1605	1161*	-0.2
HDPE-25BGPW	20	21*	243	253	21	21	2.4
HDPE-25BGPW-MAPE	27	27	288	248*	27	27	1.8
HDPE-25PW	21	22	336	291*	20	18	3.8
HDPE-25PW-MAPE	27	28*	333	304*	19	21	1.8
HDPE-40PW	20	22*	438	392*	10	10	7.2
HDPE-40PW-MAPE	34	35	494	438*	13	14	3.7

Properties are given as "Original" or un-soaked and with "soak" treatment. The asterisk "" after a value indicates significant difference between treatments ($P < 0.05$).

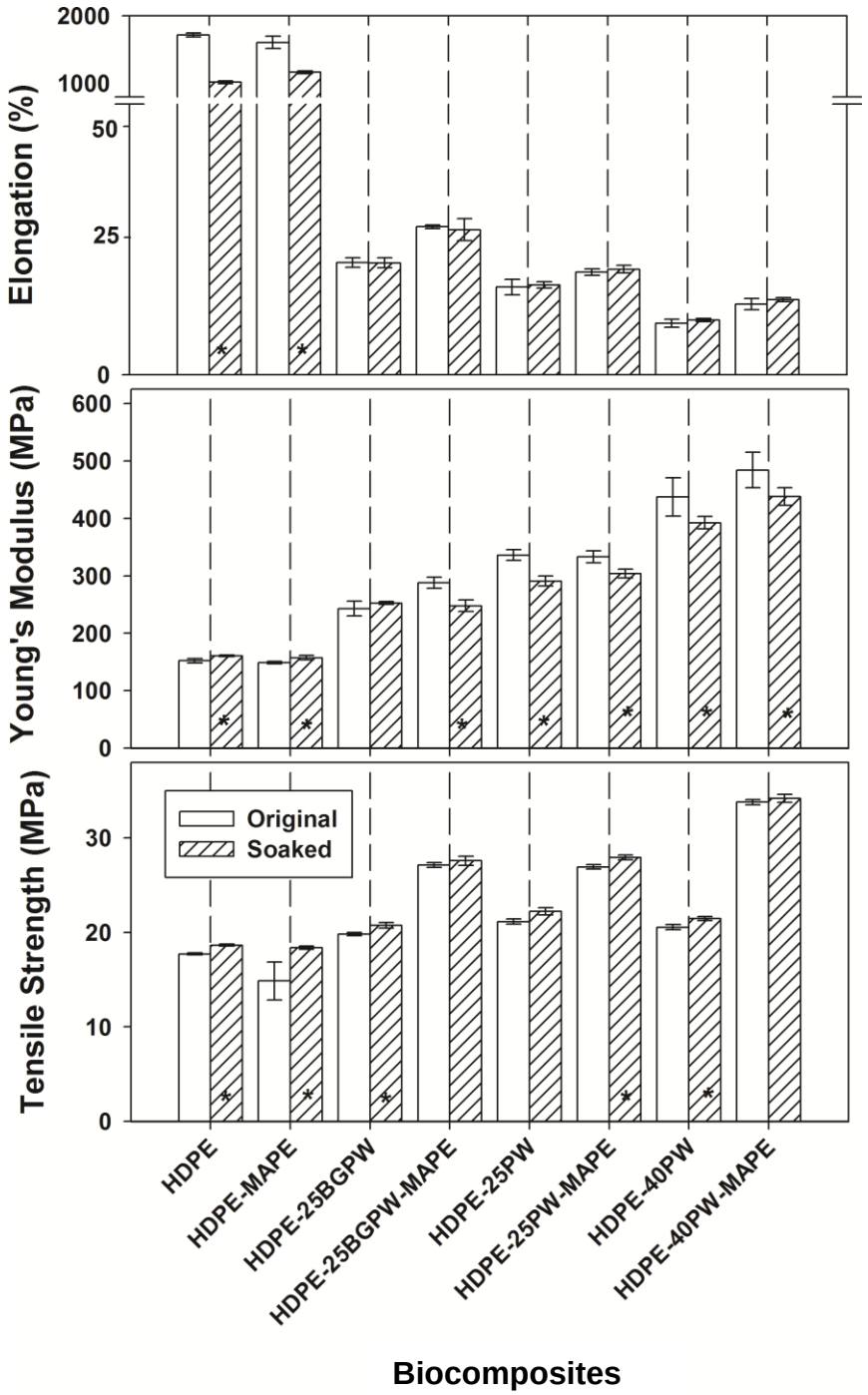

Fig. 4. Comparative mechanical properties after 672 h of soaking. The asterisk "*" indicates significant difference between treatments.

Thermal Analysis

The unique chemical and physical properties associated with wood from each species affect the thermal properties of the composite differently (Avérous and Le Digabel 2006; Kalia *et al*. 2009; Khalaf 2010). The thermal properties measured by DSC of the PW composite blends containing different concentrations of MAPE and PW

preparations are shown in Table 5. Only a single endothermic (melting) and exothermic (crystallization) peaks were observed in the DSC curves for all samples.

Table 5. DSC Thermal Data for HDPE-PW Composites

Composition	T_c (°C)	ΔH_c (J/g)	T_m (°C)	ΔH_m (J/g)	χ_c (%)
HDPE	116.72	221.9	128.4	186.9	63.8
HDPE-MAPE	116.73	230.5	128.1	204.4	69.8
HDPE-25BGPW	113.11	166.7	133.1	134.8	61.3
HDPE-25BGPW-MAPE	116.83	163.2	128.2	132.5	60.3
HDPE-25PW	113.02	148.3	132.6	128.8	58.6
HDPE-25PW-MAPE	115.58	134.2	126.6	117.9	53.7
HDPE-40PW	112.11	125.4	132.9	103.8	47.2
HDPE-40PW-MAPE	113.94	122.2	130.6	102.3	46.6

The majority of the composites exhibited a slightly higher T_m compared to the T_m of neat HDPE. This observation has been reported in other lignocellulosic plastic composites (Avérous and Le Digabel 2006; Kalia *et al*. 2009). The increase in T_m in the composites may be due to disruption of the HDPE crystal lattice network by the presence of PW particles. The addition of PW to HDPE resulted in a composite with lower crystallization (ΔH_c) and enthalpy (ΔH_m) levels compared to neat HDPE (refer to Table 5). The lowered degrees of crystallization in composite blends roughly corresponded to the concentration of the PW filler. For example, a blend containing HDPE-25PW exhibited a degree of crystallinity 8% lower than neat HDPE; and blend-containing HDPE-40PW exhibited a degree of crystallinity 26% lower than neat HDPE. The least change in degree of crystallinity occurred in the HDPE-BGPW and HDPE-BGPW-MAPE composites, which were 4 and 5% lower, respectively, compared to neat HDPE. This situation is characterized as a filler size phenomenon.

Other investigators have also observed a decrease in the crystallinity values associated with various lignocellulosic plastic composites (Kalia *et al.* 2009; Khalaf 2010). The reduction of crystallinity and enthalpy values can be explained by the amount of free volume between the polymer chains capable of allowing filler to be intermixed (Khalaf 2010). Therefore, as the volume of filler increases, less resin polymer intermolecular free volume is capable of dissipating the filler via the physical interaction between the filler and resin (Khalaf 2010). The presence of MAPE in the composite had a slightly negative affect on the crystallinity levels of the composites when compared to composites without MAPE.

It is important to determine the thermal stability of PW fillers because the temperatures employed during commercial processing, such as injection molding, may exceed 200 °C. A thermogravimetric curve is plotted in Fig. 5 to illustrate PW composites, and all PW composites results are summarized in Table 6.

As shown, the degradation of neat HDPE, occurring in a single stage, begins at 449 °C, with a maximum decomposition rate occurring at 463 °C. HDPE degradation was 99.1% complete at the end of this stage. The HDPE-MAPE blend mimics these parameters. In contrast, there were several degradation peaks associated with the PW composites, as shown in Fig. 5.

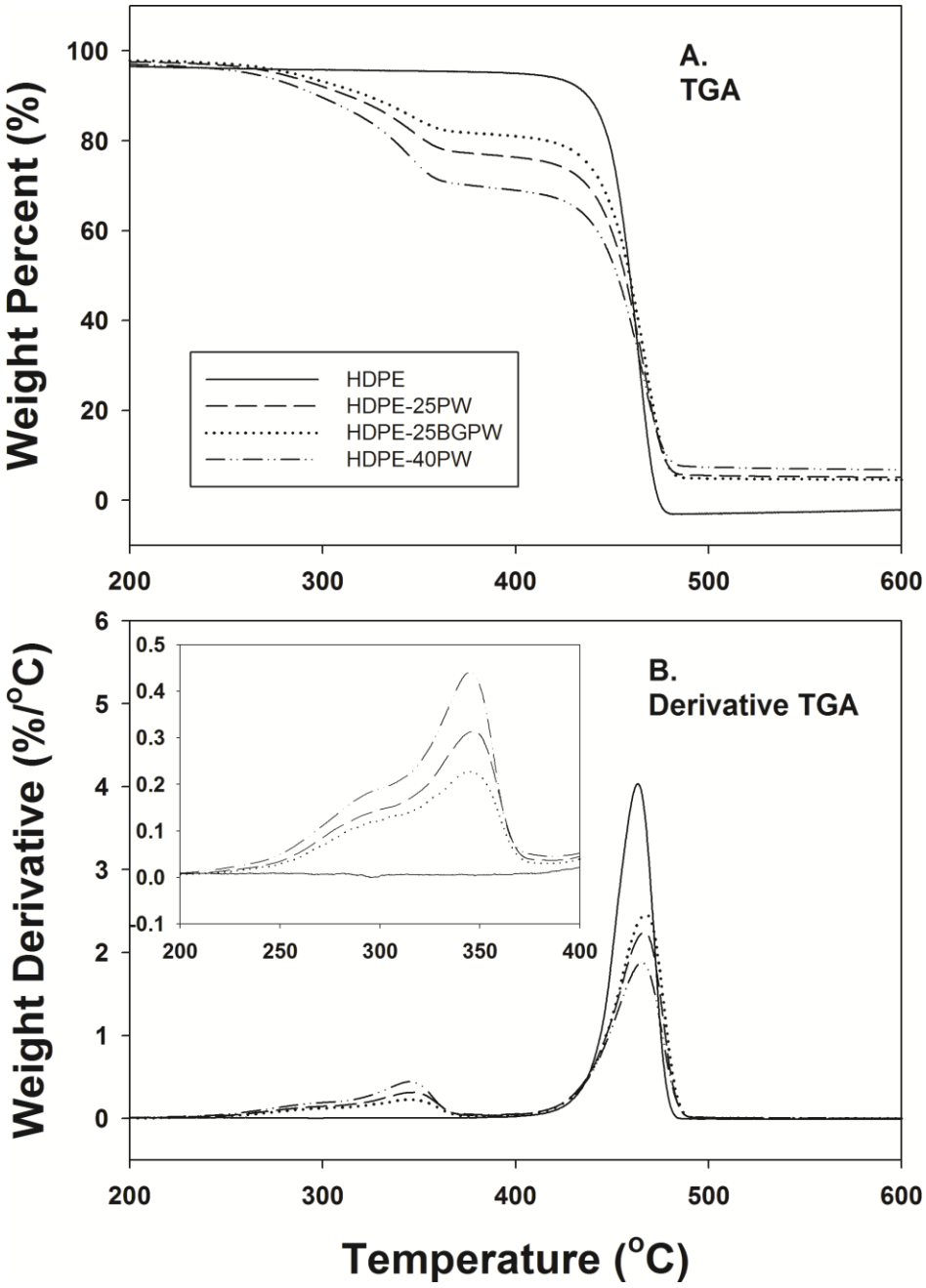

Fig. 5. TGA analysis of HDPE and HDPE-PW composites. A.) TGA profile of HDPE and HDPE-PW composites. B.) TGA derivative of HDPE and HDPE-PW composites

The insert in Fig. 5B depicts a number of overlapping peaks occurring during the degradation of PW composites; these degradation peaks obscured specific degradation events. The initial degradation temperature (T_d) of the PW flour was 215 °C and the decomposition peak occurred at ≈270 °C. This degradation peak is associated with the decomposition of low molecular weight components such as hemicellulose, which degrades between 225 to 325 °C (Lee and Wang 2006; Clemons and Stark 2009). A second higher degradation peak occurred with a maximum at 345 °C. This degradation peak is associated with decomposition of cellulose, which degrades between 300 to 400 °C (Lee and Wang 2006). A third degradation peak corresponds to lignin

decomposition and is often reported occurring near 420 ^{o}C; however it was not seen in this study (Lee and Wang 2006). It is believed this peak was obscured by the decomposition of HDPE. The increase of residual weight for the composites is due to the heterogeneous ingredients in the wood flour. Based on the TGA analysis and since the injection molding temperatures did not exceed 200 ^{o}C, the PW composites were thermally stable for the temperatures they were subjected to in this study.

Table 6. TGA Data for PW Composites

Composition	lst	2nd	Peak Temp. (^{o}C)**		Residual
	T_d (^{o}C)*	T_d (^{o}C)	Peak 1	Peak 2	(%)
HDPE	--	449	--	463	0.9
HDPE-MAPE	--	444	--	461	4.4
HDPE-25BGPW	294	448	346	467	6.6
HDPE-25BGPW-MAPE	309	443	354	465	8.7
HDPE-25PW	299	447	347	467	7.6
HDPE-25PW-MAPE	303	449	347	468	6.1
HDPE-40PW	301	446	345	465	10.1
HDPE-40PW-MAPE	306	447	347	467	10.5

*Initial thermal degradation temperature (T_d)
**Maximum degradation temperature

CONCLUSIONS

1. Paulownia wood flour filler produced composites that had comparable or superior mechanical, flexural, and impact strength properties to composites of pine wood flour filler.
2. The inclusion of a MAPE coupling agent improved the mechanical properties of the HDPE-PW composites with MAPE accounting for almost a 50% improvement in tensile strength.
3. All HDPE-PW composite blends exhibited impact energy properties that were comparable to neat HDPE. The addition of 5% by weight of a MAPE coupling agent accounted for an increase in the impact energy by as much as 30% to composites made without MAPE.
4. Particle size tests comparing blends of 25BGPW composed of particles of ≤75 µm with 25PW composed of particles of ≤590 µm showed no or little differences in terms of their mechanical or flexural properties.
5. All HDPE-PW composites soaked in water for 28 days exhibited an increase in weight gain but only slight changes to the mechanical properties occurred. Inclusion of MAPE in the composite blend decreased weight gain.

ACKNOWLEDGEMENTS

The authors acknowledge Xavier Holford, Lauren Duvall, and Kathy Hornbeck for technical assistance. This research has been supported partly through the Project Seed, American Chemical Society, Washington D.C. Mention of trade names or commercial products in this publication is solely for the purpose of providing specific information and does not imply recommendation or endorsement by the US Department of Agriculture. USDA is an equal opportunity provider and employer.

REFERENCES CITED

Anonymous. (2011). *Princess Tree*, Plant Conservation Alliance's Alien Plant Working Group, (http://www.nps.gov/plants/alien/fact/pato1.htm).

Anonymous. (2012). *Wood-Plastic Composite & Plastic Lumber to 2015*, Freedonia Group, Jan. 2012, (http://www.reportsnreports.com/reports/145422-wood-plastic-composite-plastic-lumber-to-2015.html).

Ashori, A., and Nourbakhsh, A. (2009). "Studies on Iranian cultivated paulownia – A potential source of fibrous raw material for paper industry," *Eur. J. Wood Wood Prod.* 67(3), 323-327.

Ashori, A., Sheshmani, S., and Farhani, F. (2013). "Preparation and characterization of bagasse/HDPE composites using multi-walled carbon nanotubes," *Carb. Polym.* 92(1), 865-871.

Avérous, F., and Le Digabel, F. (2006). "Properties of biocomposites based on lignocelluosic fillers," *Carb. Polym.* 66(4), 480-493.

Ayrilmis, N., and Kaymakci, A. (2013). "Fast growing biomass as reinforcing filler in thermoplastic composites: *Paulownia elongata* wood," *Ind. Crops Prod.* 4, 457-464.

Berglund, L. and Rowell, R. M. (2005). *Wood Composites, Handbook of Wood Chemistry and Wood Composites.* CRC Press, Boca Raton, Florida.

Bevill, K. (2011). "Marginal land could be significant source of biofuel crops," *Ethanol Prod. Mag.* Jan. 20, 2011, (http://www.ethanolproducer.com/articles/7428/ marginal-land-could-be-significant-source-of-biofuel-crops).

Burden, D. (2012). "Forestry profile," *Ag MRC*, (http://www.agmrc.org/commodities__products/forestry/forestry-profile/).

Carlborn, K., and Matuana, L. M. (2006). "Functionalization of wood particles through a reactive extrusion process," *J. Appl. Polym. Sci.* 101(5), 3131-3142.

Chinese Academy of Forestry Staff. (1986). *Paulownia in China: Cultivation and Utilization*, Asian Network for Biological Sciences and International Development Research Centre, Singapore.

Clemons, C. M. (2010). "Wood flour," *Functional Fillers for Plastics*, M. Xanthos (ed.), 2nd Ed., Wiley-VCH Verlag GmBH & Co., Weinheim, Germany, pp. 269-290.

Clemons, C. M., and Stark, N. M. (2009). "Feasibility of using salt cedar as a filler in injection-molded polyethylene composites," *Wood Fiber Sci.* 41(1), 2-12.

Eilperin, J. (2010). "The unintended ripples from biomass subsidy program," *The Washington Post*, Sunday, January 10, 2010, (http://www.washingtonpost.com/wp-dyn/content/article/2010/01/09/AR2010010902023. html).

Ehrenstein, G. (2001). *Functional Polymeric Materials*, Carl Hanser Verlag, Munich, Germany.

English, G. J., and Ewing, T. W. (2002). "Vision for bioenergy and biobased products in the United States." *Biomass Technical Advisory Committee, Est. by the Biomass R&D Act of 2000,* (http://www.usbiomassboard.gov/pdfs/biovision_03_webkw.pdf).

Girones, J., Menedez J. A., Boufi S., Vilaseca, F., and Mutje, P. (2007). "Effect of silane coupling agents on the properties of pine fibers/polypropylene composites," *J. Appl. Polym. Sci.* 103(6), 3706-3717.

Hristov, V. N., Vasileva, ST., Krumova, M., Lach, R., and Michler, G. H. (2004). "Deformation mechanisms and mechanical properties of modified polypropylene/ wood fiber composites," *Polym. Comp.*, 25(5), 521-526.

Joseph, P. V., Rabello, M. S., Mattoso, L. H. C., Joseph, K., and Thomas, S. (2002). "Environmental effects on the degradation behavior of sisal fiber reinforced polypropylene composites," *Comp. Sci. Technol.* 62(10-11), 1357-1372.

Joshee, N. (2012). "Paulownia: A multipurpose tree for rapid lignocellulosic biomass production," In: *Handbook of Bioenergy Crop Plants*, C. Kole, C. P. Joshi, and D. Shonnard (eds.), Taylor & Francis Inc., Boca Raton, Florida, pp. 671-686.

Kalia, S., Kaith, B. S., and Kaur, I. (2009). "Pretreatment of natural fibers and their application as reinforcing material in polymer composites-a review," *Polym. Eng. Sci.* 49(7), 1253-1272.

Karmarkar, A., Chauhan, S. S., Modak, J. M., and Chanda, M. (2007). "Mechanical properties of wood–fiber reinforced polypropylene composites: Effect of a novel compatibilizer with isocyanate functional group," *Comp. Part A.* 38A, 227-233.

Khalaf, M. N. (2010). "Effect of alkali lignin on heat of fusion, crystallinity and melting points of low density polyethylene (LDPE), medium density polyethylene (MDPE) and high density polyethylene (HDPE)," *J. Thi-Qar Sci.* 2(2), 89-95.

Lee, S.-H., and Wang, S. (2006). "Biodegradable polymers/bamboo fiber biocomposite with bio-based coupling agent," *Comp. Part A.* 37(1), 80-91.

LeVan-Green, S. L., and Livingston, J. (2001). "Exploring the uses for small-diameter trees," *J. For. Prod.*, 51(9), 10-21.

Lei, Y., Wu, Q., Clemons, C. M., Yao, F., and Xu, Y. (2007). "Influence of nanoclay on properties of HDPE/wood composites," *J. Appl. Polym. Sci.* 106(6), 3958-3966.

Lopez, J. L., Sain, M., Cooper, P. (2006). "Performance of natural-fiber-plastic composites under stress for outdoor applications: Effect of moisture, temperature, and ultraviolet light exposure," *J. Appl. Polym. Sci.* 99(3), 2570-2577.

Millman, J. (2008). "Sawdust shock: A shortage looms as economy slows," *The Wall Street Journal*, Monday, March 3, 2008, (http://online.wsj.com/article/SB120451039119406735.html).

Myers, G. C., Barbour, R. J., and AbuBakr, S. M. (2003). "Small-diameter trees used for chemithermomechanical pulps," USDA, Forest Service; 12 p. General Technology Report No.: FPL-GTR-141.

Myers, G. E., Chahyadi, I. S., Gonzalez, C., Coberly, C. A., and Ermer, D. S. (1991). "Wood flour and polypropylene or high-density polyethylene composites: Influence of maleated polypropylene concentration and extrusion temperature on properties," *Intern. J. Polym. Mater.* 15(3-4), 171-186.

Ramaraj, B. (2007). "Mechanical and thermal properties of polypropylene/sugarcane bagasse composites," *J. Appl. Polym. Sci.* 103(6), 3827-3832.

Stark, N. M., and Berger, M. J. (1997). "Effect of particle size on properties of wood flour reinforced polypropylene composites," In: *4th International Conference on. Woodfiber-Plastic Composites,* Madison, WI, 12-14 May, Pp. 134-143.

Stark, N. M., and Mueller, S. A. (2008). "Improving the color stability of wood-plastic composites through fiber pre-treatment," *Wood Fiber Sci.* 40(2), 271-278.

Thomason, J. L. and Vlug, M. A. (1997). "Influence of fibre length and concentration on the properties of glass fibre-reinforced polypropylene: 4. Impact Properties," *Comp. Part A* 28A, 277-288.

Thwe, M. M., and Liao, K. (2002). "Effects of environmental aging on the mechanical properties of bamboo—glass fiber reinforced polymer matrix hybrid composites." *Comp. Part A.* 33(1), 43-52.

Xu, T., Yu, J., and Jin Z. (2001). "Effects of crystalline morphology on the impact behavior of polypropylene," *Materials and Design* 22(1), 27-31.

Zabihzadeh, S. M. (2010). "Flexural properties and orthotropic swelling behavior of bagasse/thermoplastic composites," *BioResources* 5(2), 650-660.

Zahedi, M., Tabaras, T., Ashori, A., Madhoushi, M., and Shakeri, A. (2012). "A comparative study on some properties of wood plastic composites using canola stalk, Paulownia, and Nanoclay," *J. Appl. Polym. Sci.* 129(3), 1491-1498.

Article submitted: April 18, 2013; Peer review completed: June 7, 2013; Revised version accepted: July 10, 2013; Published; July 17, 2013.